

Synthesis, Crystal Structures and Magnetic Characterization of Two Pyridinecarboxamide *trans*-Dicyanideiron(III) Building Blocks

XIA CHEN¹, LINGQIAN KONG², HONGYAN ZHANG¹ and DAOPENG ZHANG^{1,*}

¹College of Chemical Engineering, Shandong University of Technology, Zibo 255049, P.R. China

²Dongchang College, Liaocheng University, Liaocheng 252059, P.R. China

*Corresponding author: E-mail: dpzhang73@126.com

Received: 11 October 2014;

Accepted: 18 December 2014;

Published online: 26 May 2015;

AJC-17259

Two *trans*-dicyanometalates based-on quasi-planar tetradentate chelating pyridinecarboxamide ligand with the formula $[\text{H}_3\text{O}][\text{Fe}(\text{bpb})(\text{CN})_2] \cdot 2.5\text{H}_2\text{O}$ (**1**) and $[\text{H}_3\text{N}(\text{CH}_2)_3\text{NH}_3]_{0.5}[\text{Fe}(\text{bpb})(\text{CN})_2] \cdot 2\text{H}_2\text{O}$ (**2**) ($\text{bpb}^{2-} = 1,2\text{-bis}(\text{pyridine-2-carboxamido})\text{benzenate}$) has been obtained, structurally and magnetically characterized. Single X-ray diffraction reveals their same anionic mononuclear structure, in which the Fe(III) ion is six-coordinated with the four equatorial positions occupied by a N_4 unit of the pyridinecarboxamide ligand and two axial ones from two C atoms of the cyanide groups. Magnetism characterization for these two compounds show the typical paramagnetic characteristic of the low-spin iron(III) ion.

Keywords: Cyanide precursor, Synthesis, Crystal structure, Magnetic property.

INTRODUCTION

During the past several decades, cyano-bridged transition metal systems have always been the subject in the coordination chemistry field¹⁻⁴ not only because of their various structure types from polynuclear clusters to three-dimensional networks but also for their interesting functional properties, including molecular sieves⁵⁻⁸, hosts for small molecules and ions⁹, catalysts for the production of ether polyols or polycarbonates¹⁰, room temperature magnets¹¹⁻¹⁵, electrochemically tunable magnets^{16,17}, photo-magnetic materials and magneto-optical effect^{18,19}. The rational design of cyanide-bridged materials can be achieved following a building-block approach with the premeditated association of various complexes and capped polycyanidometallates $[\text{M}(\text{L})_x(\text{CN})_y]^{z-}$ (L = mono- or multi-dentate ligand). This strategy provides better control of the dimensionality of the final outcome when carefully selecting the building blocks of both the negative charged $[\text{M}(\text{L})_x(\text{CN})_y]^{z-}$.

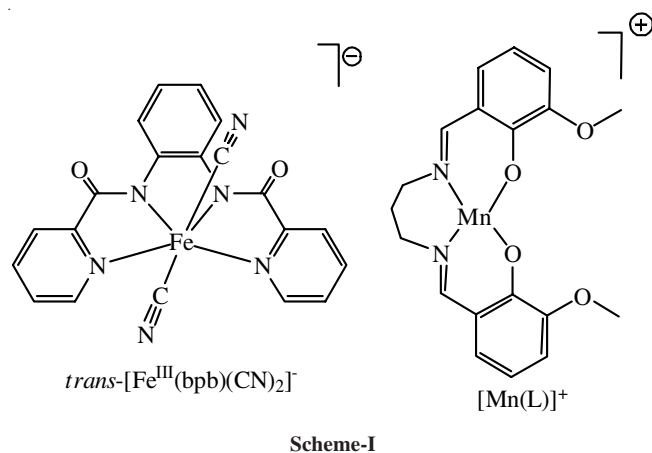
In recent years, our group have focused on the controllable synthesis of low-dimensional cyanide-bridged magnetic complexes, which can maybe show interesting magnetic properties, for examples single molecular magnet (SMM) and single chain magnet (SCM), through rational design and selection of cyanide-containing building blocks with two *trans* cyanide groups based-on quasi-planar tetradentate chelating pyridinecarboxamide ligand²⁰⁻²⁷. These types of cyanide precursors with relative large equatorial steric effect can effectively lower the

dimensionality, therefore weakening of the intermolecular magnetic interaction. For the purpose of increasing solubility of the cyanide precursor $\text{K}[\text{Fe}(\text{bpb})(\text{CN})_2]$ in weak polar solvents, which can in turn facilitate the synthesis of cyanide-bridged complexes in organic environment, we carried out the metathesis reaction of $\text{K}[\text{Fe}(\text{bpb})(\text{CN})_2]$ with Et_4NCl and also *in situ* with $[\text{Mn}(\text{L})(\text{H}_2\text{O})_2]\text{ClO}_4$ [L = $\text{N,N}'\text{-}(1,3\text{-propylene})\text{-bis}(3\text{-methoxysalicylideneimine})$, ($\text{bpb} = 1,2\text{-bis}(\text{pyridine-2-carboxamido})\text{benzenate}$)] (**Scheme-I**). Unexpectedly, two dicyanoiron(III) ion-pair compounds with the formula $[\text{H}_3\text{O}][\text{Fe}(\text{bpb})(\text{CN})_2] \cdot 2.5\text{H}_2\text{O}$ (**1**) and $[\text{H}_3\text{N}(\text{CH}_2)_3\text{NH}_3]_{0.5}[\text{Fe}(\text{bpb})(\text{CN})_2] \cdot 2\text{H}_2\text{O}$ (**2**) were obtained, for which the synthesis, crystal structures and magnetic character described in present paper.

EXPERIMENTAL

All the reactions were carried out under an air atmosphere and all chemicals and solvents used were reagent grade without further purification. The cyanide precursor $\text{K}[\text{Fe}(\text{bpb})(\text{CN})_2]$ was synthesized according to the reported method²⁸.

Preparation of compound (1): $\text{K}[\text{Fe}(\text{bpb})(\text{CN})_2]$ (1 mmol, 465 mg) was dissolved in distilled water (30 mL) and Et_4NCl (1 mol, 166 mg) was added. The suspension was stirred for about 2 h before the dark-brown solid formed was collected by filtration. Single crystals suitable for X-ray diffraction were obtained by dissolving the solid in methanol layered ether after



one month. Yield: 35.6 mg, 73 %. Anal. Calcd. for $C_{20}H_{20}N_6O_{5.5}Fe$: C, 49.20; H, 4.13; N, 17.21; found: C, 49.01; H, 3.68; N, 17.58.

Preparation of compound 2: The methanol suspension containing $K[Fe(bpb)(CN)_2]$ (0.1 mmol, 46.5 mg) and Et_4NCl (0.1 mol, 16.6 mg) was stirred for about 2 h before the undissolved materials were removed by filtration. To the filtrate, $[Mn(L)(H_2O)_2]ClO_4$ (58.8 mg, 0.10 mmol) in methanol (10 mL) was added under the stirring condition and the resulting solution was kept undisturbed at room temperature. After one week, dark-brown block crystals were collected by filtration with the yield about 35 % based-on $K[Fe(bpb)(CN)_2]$. Anal. Calcd. for $C_{21.5}H_{22}N_7O_4Fe$: C, 51.82; H, 4.45; N, 19.68; found: C, 51.54; H, 3.83; N, 19.46.

Physical measurements: Elemental analyses of carbon, hydrogen and nitrogen were carried out with an Elementary Vario El. Variable-temperature magnetic susceptibility was performed on a Quantum Design MPMS SQUID magnetometer.

Structure determination: Data were collected on a Oxford Diffraction Gemini E diffractometer with MoK_{α} radiation ($\lambda = 0.71073 \text{ \AA}$) at 293 K. Final unit cell parameters were derived by global refinements of reflections obtained from integration of all the frame data. The collected frames were integrated by using the preliminary cell-orientation matrix. CrysAlisPro Agilent Technologies software was used for collecting frames of data, indexing reflections and determination of lattice constants; CrysAlisPro Agilent Technologies for integration of intensity of reflections and scaling, SCALE3 ABSPACK for absorption correction, The structures were solved by the direct method (SHELXS-97) and refined by full-matrix least-squares (SHELXL-97) on F^2 .²⁹ Anisotropic thermal parameters were used for the non-hydrogen atoms and isotropic parameters for the hydrogen atoms. Hydrogen atoms were added geometrically and refined using a riding model. Crystallographic data and experimental details for structural analyses are summarized in Table-1. CCDC: 1028590-1028591.

RESULTS AND DISCUSSION

Some important structural parameters for compounds **1** and **2** are collected in Table-2. The anionic structure for the compounds **1** and **2** is shown in Fig. 1 and their supramolecular structure formed by intermolecular hydrogen bond interactions are shown in Figs. 2 and 3, respectively.

TABLE 1
CRYSTALLOGRAPHIC DATA AND STRUCTURE
REFINEMENT SUMMARY FOR THE COMPOUNDS 1 AND 2

	1	2
Empirical formula	$C_{20}H_{20}N_6O_{5.5}Fe$	$C_{21.5}H_{22}N_7O_4Fe$
Formula weight	488.27	498.31
Temperature (K)	293	293
Wavelength (\AA)	0.71073	0.71073
Crystal system	Monoclinic	Monoclinic
Space group	C2/c	C2/c
Unit cell dimensions (\AA)	a = 27.266(4) b = 12.7163(16) c = 19.127(3)	a = 26.6157(11) b = 12.6487(4) c = 19.1944(7)
β ($^\circ$)	133.934(4)	133.669(4)
Volume (\AA^3)	4775.7(11)	4674.1(3)
Z	8	8
Calculated density (mg/m^3)	1.358	1.416
Absorption coefficient	0.675	0.688
F(000)	2016	2064
Reflections/collected/unique	8677/4100	28086/4116
Data/restraints/parameters	4100/0/294	4116/0/304
Goodness-of-fit on F^2	1.034	1.090
Final R indices [$I > 2\sigma(I)$]	0.0786	0.0625
R indices (all data)	0.2364	0.2040
Largest diff. peak and hole ($e/\text{\AA}^3$)	1.362 and -	1.370 and -1.263

TABLE-2
SELECTED BOND LENGTHS (\AA) AND ANGLES ($^\circ$)
FOR THE COMPOUNDS 1 AND 2

	1	2
Fe(1)-C(1)	1.970(6)	1.972(5)
Fe(1)-C(2)	1.973(5)	1.970(5)
Fe(1)-N(3)	1.904(4)	1.885(3)
Fe(1)-N(4)	1.884(4)	1.897(3)
Fe(1)-N(5)	2.004(4)	2.005(3)
Fe(1)-N(6)	2.005(4)	2.004(3)
C(2)-Fe(1)-C(1)	171.5(2)	170.72(19)
N(1)-C(1)-Fe(1)	178.1(5)	179.0(4)
N(2)-C(2)-Fe(1)	178.3(4)	178.4(5)

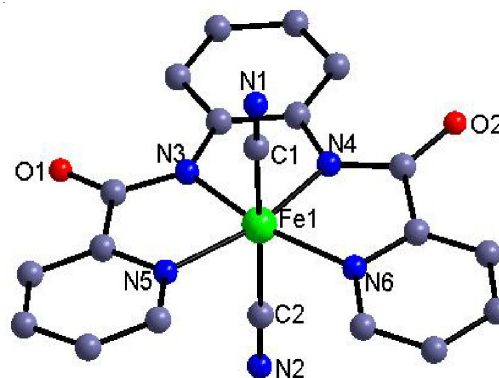


Fig. 1. Anionic molecular structure of compounds **1** and **2**. The balanced cation, the solvent water molecules and all the H atoms have been omitted for clarity

As can be found in Table-2, these two compounds crystallize both in monoclinic space group $P2(1)/n$ and contain eight independent units in the unit cell. The Fe atom is coordinated by four N atoms of pyridinecarboxamide ligand locating in the equatorial plane and two C atoms of cyanide groups in *trans* position, forming a slightly distorted octahedral geometry. The Fe-N bond length is in the range of 1.885(3)-2.005(4) \AA for

these two compounds and the Fe-C_{cyanide} bond length is distributed to the narrow range of 1.970(5)-1.973(5) Å. The mean deviation of the plane formed by FeN₄ unit is 0.0262 and 0.0335 Å and the Fe ion is only out of the plane 0.0014 and 0.0033 Å, respectively, indicating clearly that these five atoms are in a perfect equatorial plane. As listed in Table-2, the bond angle of Fe-C=N in the realm of 172.0(9)-177.4(6)° demonstrates that the three atoms are in a good linear configuration. It should be pointed out, under the help of the abundant intermolecular O...H...O and O...H...N hydrogen interactions, these two can be linked into 2D and 3D supramolecular structures, respectively (Figs. 2 and 3).

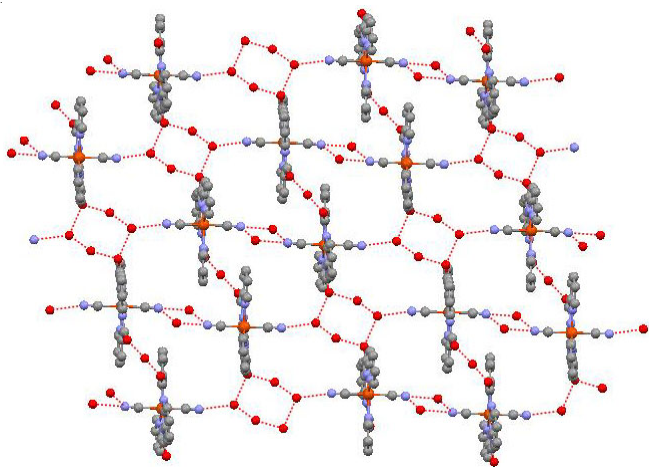


Fig. 2. 2D supramolecular structure of compound **1** formed by the intermolecular H-bond interactions

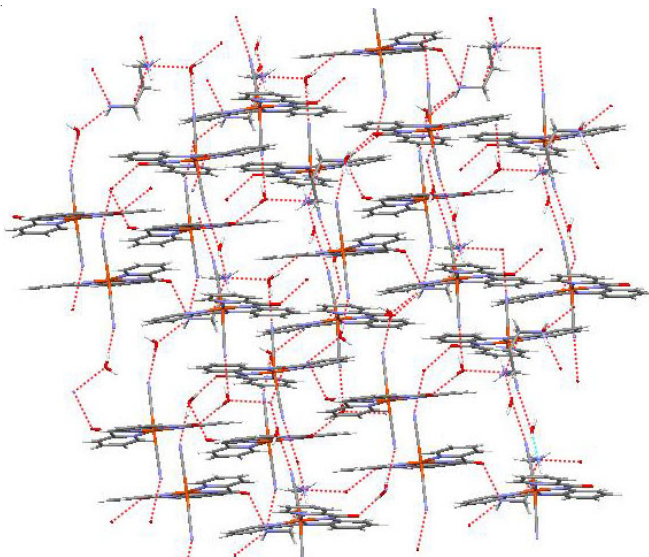


Fig. 3. 3D supramolecular structure of compound **2** formed by the intermolecular H-bond interactions

The magnetic characteristic of these two compounds has been studied with compound **1** as representative. The temperature dependence of magnetic susceptibility for compound **1** measured in the range of 2-300 K under an external magnetic field of 2000 Oe is illustrated in Fig. 4. The $\chi_M T$ value at room temperature is 0.53 emu K mol⁻¹, higher than the low-spin Fe(III) value of 0.375 K mol⁻¹, which can be attributed to the spin-orbital coupling. With the temperature lowering, the $\chi_M T$

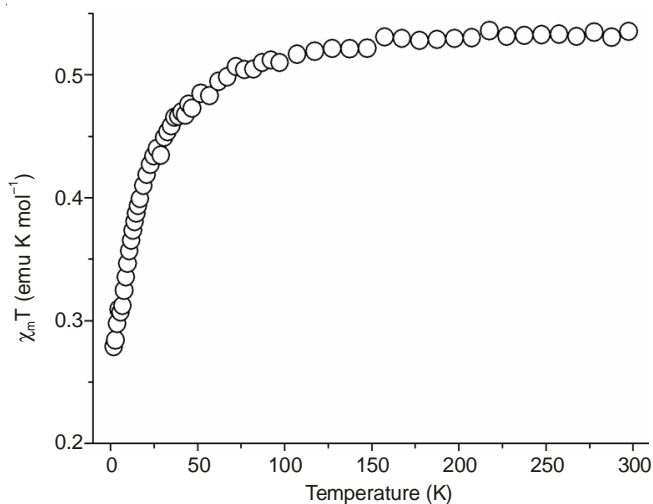


Fig. 4. Temperature dependence of $\chi_M T$ of compound **1**

value decreases with a very low speed up to about 50 K and then decreases with a high speed and reaches the value of about 0.27 emu K mol⁻¹ at 2 K. The magnetic behavior of compound **1** is typical characteristic of low spin Fe(III) ion, which is similar to that for the reported low-spin mononuclear Fe(III) compounds^{30,31}.

ACKNOWLEDGEMENTS

This work was supported by the Natural Science Foundation of China (21171107) and the Natural Science Foundation of Shandong Province (ZR2011BM008) and the Science and Technology Project of High Education, Shandong Province (No. J11LB09).

REFERENCES

1. K.R. Dunbar and R.A. Heintz, *Prog. Inorg. Chem.*, **57**, 155 (2009).
2. H. Miyasaka, A. Saitoh and S. Abe, *Coord. Chem. Rev.*, **251**, 2622 (2007).
3. L.M.C. Beltran and J.R. Long, *Acc. Chem. Res.*, **38**, 325 (2005).
4. S. Wang, X.H. Ding, J.L. Zuo, X.Z. You and W. Huang, *Coord. Chem. Rev.*, **255**, 1713 (2011).
5. D. Williams, J. Kouvetakis and M. O'Keefe, *Inorg. Chem.*, **37**, 4617 (1998).
6. M.P. Shores, L.G. Beauvais and J.R. Long, *J. Am. Chem. Soc.*, **121**, 775 (1999).
7. M.P. Shores, L.G. Beauvais and J.R. Long, *Inorg. Chem.*, **38**, 1648 (1999).
8. M.V. Bennett, L.G. Beauvais, M.P. Shores and J.R. Long, *J. Am. Chem. Soc.*, **123**, 8022 (2001).
9. K.K. Klausmeyer, T.B. Rauchfuss and S.R. Wilson, *Angew. Chem. Int. Ed.*, **37**, 1694 (1998).
10. D.J. Darensbourg and A.L. Phelps, *Inorg. Chim. Acta*, **357**, 1603 (2004).
11. T. Mallah, S. Thiebaut, M. Verdaguer and P. Veillet, *Science*, **262**, 1554 (1993).
12. R. Garde, F. Villain and M. Verdaguer, *J. Am. Chem. Soc.*, **124**, 10531 (2002).
13. W.R. Entley and G.S. Girolami, *Science*, **268**, 397 (1995).
14. S.M. Holmes and G.S. Girolami, *J. Am. Chem. Soc.*, **121**, 5593 (1999).
15. W.E. Hatlevik, J. Buschmann, J.L. Zhang, J.S. Manson and J.S. Miller, *Adv. Mater.*, **11**, 914 (1999).
16. O. Sato, T. Iyoda, A. Fujishima and K. Hashimoto, *Science*, **271**, 49 (1996).
17. O. Sato, S. Hayami, Y. Einaga and Z.Z. Gu, *Bull. Chem. Soc. Jpn.*, **76**, 443 (2003).
18. O. Sato, T. Iyoda, A. Fujishima and K. Hashimoto, *Science*, **272**, 704 (1996).
19. M. Mizuno, S. Ohkoshi and K. Hashimoto, *Adv. Mater.*, **12**, 1955 (2000).
20. Z.H. Ni, H.Z. Kou, Y.H. Zhao, L. Zheng, R.J. Wang, A.L. Cui and O. Sato, *Inorg. Chem.*, **44**, 2050 (2005).
21. Z.H. Ni, L.F. Zhang, V. Tangoulis, W. Wernsdorfer, A.L. Cui, O. Sato and H.Z. Kou, *Inorg. Chem.*, **46**, 6029 (2007).

22. Z.H. Ni, H.Z. Kou, L.F. Zhang, C. Ge, A.L. Cui, R.J. Wang, Y. Li and O. Sato, *Angew. Chem. Int. Ed.*, **44**, 7742 (2005).
23. Z.H. Ni, J. Tao, W. Wernsdorfer, A.L. Cui and H.Z. Kou, *Dalton Trans.*, 2788 (2009).
24. D.P. Zhang, H.L. Wang, L.J. Tian, H.Z. Kou, J.Z. Jiang and Z.H. Ni, *Cryst. Growth Des.*, **9**, 3989 (2009).
25. D.P. Zhang, Z.D. Zhao, P. Wang and Z.H. Ni, *CrystEngComm*, **15**, 2504 (2013).
26. D.P. Zhang, H.L. Wang, Y.T. Chen, Z.H. Ni, L.J. Tian and J.Z. Jiang, *Inorg. Chem.*, **48**, 5488 (2009).
27. D.P. Zhang, W.J. Si, P. Wang, X. Chen and J.Z. Jiang, *Inorg. Chem.*, **53**, 3494 (2014).
28. M. Ray, R. Mukherjee, J.F. Richardson and R.M. Buchanan, *J. Chem. Soc., Dalton Trans.*, **16**, 2451 (1993).
29. G.M. Sheldrick, SHELXTL97, Program for the Refinement of Crystal Structure, University of Göttingen, Germany (1997).
30. J.I. Kim, H.S. Yoo, E.K. Koh, H.C. Kim and C.S. Hong, *Inorg. Chem.*, **46**, 8481 (2007).
31. D.P. Zhang, S.P. Zhuo, P. Wang, X. Chen and J.Z. Jiang, *New J. Chem.*, **38**, 5470 (2014).